2019 SECED Conference
Earthquake risk and engineering towards a resilient world
9-10 September 2019, Greenwich, London

NUMERICAL ANALYSIS APPROACH BASED ON EFFECTIVE PIER STIFFNESS FOR BRIDGES WITH UNEQUAL PIER HEIGHTS

Nikolaos KARAMICHALIS[1] & Simon Mathias GREN[2]

Abstract: *The current seismic concept rules for bridges crossing steep sided valleys suggest that for shorter piers, bearings allowing movement in the transverse direction may be used. For longer piers cracked section properties can be used when performing the analyses. This is usually implemented along the full pier height and among all piers. For this approach to provide a realistic calculation of the structural period the longer piers must be of equal or approximately equal height. A numerical approach is proposed for irregular bridges where all piers are discretised into segments and a ratio of $I_{cracked\text{-}section}$ over $I_{gross\text{-}section}$ is assumed for initial response spectrum analysis. The fundamental period cracked section properties are calculated per pier segment from the secant stiffness at the theoretical yield point and are then input back into the analysis for a repetition. Iterations continue until the $I_{cracked\text{-}section}$ over $I_{gross\text{-}section}$ ratios converge within all segments, the point at which all piers have reached their effective flexural stiffness. The provided reinforcement can be used to control the pier flexural stiffness and to a certain extent control the structural period. A ductile design approach can be followed implementing a ductility behaviour factor in the response spectrum. The proposed design approach is illustrated by an example of an irregular bridge. The results are compared with results from a response spectrum analysis where cracked section properties are implemented over the full height of the piers, and a push over analysis in the transverse direction.*

Introduction

The two main challenges for an optimum deck-pier articulation for bridges resisting seismic loading are the accommodation of uniform thermal expansion and contraction of the deck, and the distribution of the seismic force among the piers. When the bridge has equal or approximately equal pier heights then the simplest option is for the seismic loading to be resisted by the piers acting as cantilevers in the transverse direction, and by the deck-pier frame in the longitudinal direction. For bridges with unequal pier heights the difficulty arises in both horizontal directions as the shorter piers attract considerably higher seismic loading than the longer piers due to their substantially increased flexural stiffness.

BS EN 1998-2 recognises this difficulty and for bridges crossing steep sided valleys proposes the use of elastomeric bearings for shorter piers to avoid the unfavourable transverse seismic action distribution among the piers. Even though this may solve partially the analysis problem, the introduction of bearings increases the construction complexity and adds a maintenance requirement for their replacement at areas away from the abutments that are inaccessible, or accessible with difficulty.

A numerical approach is presented which is advantageous when a monolithic or a restraint connection between the deck and the piers is selected for the structural system regardless of the pier heights, assuming that the accommodation of thermal effects is designable for the continuous deck length in consideration. The principle of this approach is that every pier is discretised in several segments and the effective flexural pier section stiffness represented by the ratio of cracked section moment of inertia I_{cr} over the gross section moment of inertia I_{gr} is calculated per pier segment. After an initial calculation using a response spectrum dynamic analysis the ratios are updated and input back in the analysis for a repetition until convergence is reached for all piers. The effective flexural stiffness for reinforced concrete piers is calculated based on the

[1] Principal Engineer, Major Crossings, Ramboll, Southampton, UK, nikolaos.karamichalis@ramboll.co.uk
[2] Engineer, Major Crossings, Ramboll, Copenhagen, Denmark

secant stiffness at the theoretical yield point of the reinforcement of the section of each segment. As per BS EN 1998-2 Annex C, the formula used to estimate the value of I_{cr} is given below:

$$I_{cr} = \frac{M_y}{E_c \phi_y} \quad (1)$$

where M_y is the bending moment value at the first yield of reinforcement, Φ_y is the corresponding curvature and E_c is the elastic modulus of concrete. The effective flexural stiffness assignment per pier segment allows redistribution of the seismic force among the piers between analysis iterations. As a result, every pier segment can have its own reinforcement ratio leading to an economical design as the reinforcement demand is dependent on the level of cracking.

This numerical analysis method (Analysis A) is presented by the aid of an example on a ductile bridge structure assuming a force-based design approach. The results are compared with the results of a single analysis (Analysis B) assuming the same effective flexural stiffness assigned uniformly along the full height of all piers. In addition, the results are benchmarked with the results of an equivalent displacement-based design approach assessing the seismic behaviour in the transverse direction by using a push-over analysis (Analysis C).

Bridge example

Geometry and materials

A six-span continuous post tensioned concrete box girder bridge is selected carrying a typical three-lane carriageway with spans of 50m+4x60m+50m and with pier heights of 10m, 12.5m, 16m, 12.5m and 10m. The pier cross section consists of a rectangular solid section of 1.6m by 3m with the longer section dimension aligned with the transverse bridge direction. The selection of pier heights is done to achieve a double flexural stiffness between shorter to longer pier. The concrete grade for the substructure is selected as C40/50 and the steel grade as B500c.

All deck to pier connections are monolithic with the end spans resting on sliding bearings at the abutments, where a shear key is assumed to resist the transverse seismic loading. The piers are assumed to be fixed at the base. The analysis model, the global geometry dimensions and the deck and pier cross sections with dimensions are illustrated in Figure 1.

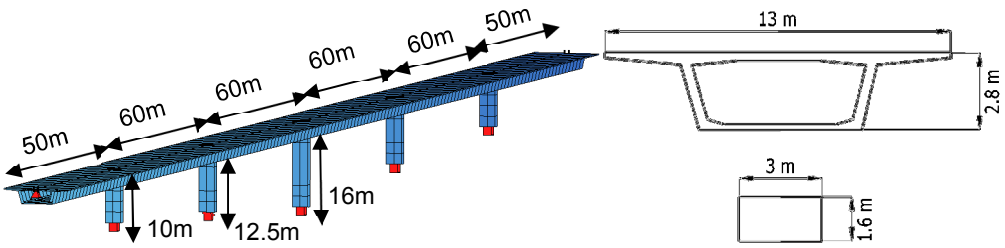

Figure 1: Bridge example global geometry and typical deck/pier cross sections

Seismic loading

Type 1 design spectrum of BS EN 1998-1 Clause 3.2.2.5 is used in the horizontal direction assuming soil type B for very dense sand founding soil. The behaviour factor is taken as q=3.5 for the reinforced concrete piers in both horizontal directions as per Clause 4.1.6 of BS EN 1998-2. In the vertical direction the spectrum of Clause 3.2.2.3 of BS EN 1998-1 is used assuming a behaviour factor of q=1.5. The peak ground acceleration is taken as 0.36*g for a 10% probability of exceedance in 50 years and an importance factor of γ_I = 1.30 is introduced for a bridge of critical importance in accordance with the provisions of BS EN 1998-2. The two design spectra are shown in Figure 2.

The deck of the bridge has an average self-weight (G) of 195 KN/m whilst the superimposed dead load and the quasi permanent component of the traffic loading (G'+ψ_2*Q) is taken as 60 KN/m.

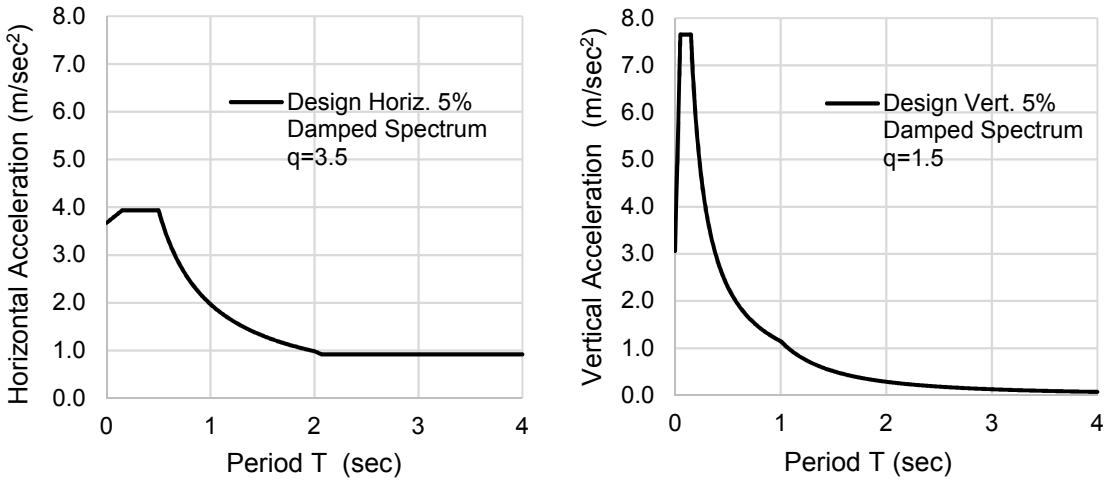

*Figure 2: BS EN 1998-1 Design Horiz. and Vertical Spectra with PGA = 1.3*0.36g, Soil type B*

Dynamic analysis and seismic loading combination

A linear dynamic (modal) analysis is undertaken in the structural software Sofistik (2016) using the ordinates of the design response spectra. The modal responses are combined using the complete quadratic combination (CQC) method and the combination of the seismic action components Ex, Ey and Ez is done in accordance with the provisions of Clause 4.2.1.4 of BS EN 1998-2 using the 30% rule.

The seismic loading combination is considered as per Clause 5.5 of BS EN 1998-2. Even though the structural system will be subject to time dependent effects for the calculation of non-seismic internal forces, the seismic analysis is undertaken on a cast 'in-place' model that excludes action effects from imposed deformations in accordance with Clause 5.5(2)P of BS EN 1998-2.

Analysis A: Pier effective flexural stiffness from iterations

Segment length

The piers are divided into segments to capture the difference in cracking along their height. The accuracy of the analysis increases with the number of segments; however, a reasonable assumption needs to be made up front to reduce the computational time and manage more easily the analysis data during the iterations. For the bridge example every pier is divided into five segments, or alternatively a convergence analysis can be adopted to find the optimum number of segments. The latter however is time consuming and for bridge piers acting as cantilevers or being part of a frame, it is known that higher moments are observed at top and bottom. As the areas of interest are close to the pier ends, two shorter segments are selected at the top and two at the bottom leaving a central segment in the middle. The length of the shorter segments may be taken as the length of the plastic hinge which can be estimated from standard textbook formulas such as the one proposed in Priestley et. al. (1996). In the present study the two-plus-two end shorter pier segments are taken as 2m, a value which is between the longer and shorter dimension of the pier section. The segment lengths are shown in Table 1.

Initial flexural stiffness and reinforcement ratio

The initial flexural stiffness can be taken from the section gross second moment of inertia, or from the average value between the cracked and the gross cross section properties. From experience it is known that either of these two values will yield conservative initial results and will increase the analysis iterations. A reasonable initial assumption of the cracked section properties is for the ratio of I_{cr}/I_{gr} to start at a value of 0.50.

An initial estimate is also required for the amount of reinforcement in every segment. Higher reinforcement ratios will tend to increase the effective flexural stiffness however it is found preferable to start at a lower value and then increase the reinforcement through the iterations to reach convergence. The longitudinal reinforcement ratios can typically start with a minimum value of ρ=1%. The flexural capacity of every segment is the indication of how far a converged solution from a current iteration is. If the reinforcement is increased within an iteration at one pier then this

pier will attract more seismic force in the next iteration and so on. As a result, the reinforcement increment steps need to take place with economy to balance between satisfying the strength requirements and the increase in stiffness. The initial I_{cr}/I_{gr} and reinforcement ratios are shown in Table 1.

	Piers 1/5			**Piers 2/4**			**Pier 3**		
Segment	L (m)	I_{cr}/I_{gr}	ρ (%)	L (m)	I_{cr}/I_{gr}	ρ (%)	L (m)	I_{cr}/I_{gr}	ρ (%)
1	2	0.50	1.00	2	0.50	1.00	2	0.50	1.00
2	2	0.50	1.00	2	0.50	1.00	2	0.50	1.00
3	2	0.50	1.00	4.5	0.50	1.00	8	0.50	1.00
4	2	0.50	1.00	2	0.50	1.00	2	0.50	1.00
5	2	0.50	1.00	2	0.50	1.00	2	0.50	1.00

Table 1. Pier segment lengths, initial I_{cr}/I_{gr} ratios and longitudinal reinforcement ratios

Analysis results and discussion

The first two oscillation modes are translational and are shown in Figure 3. The analysis is undertaken for the seismic combination transverse bending moment at the base of the piers as this bending moment is usually higher than the equivalent longitudinal bending moment where the piers are part of a frame. After the convergence of the seismic forces in the transverse direction it is verified that the seismic design is valid also in the longitudinal direction.

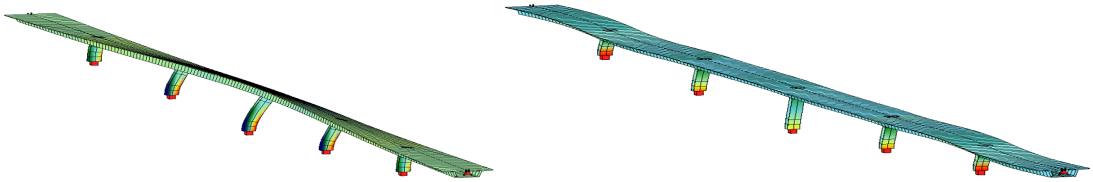

Figure 3: 1st mode shape at period T_1 (transverse) and 2nd mode shape at period T_2 (longit.)

The results of the first analysis iteration are presented in Table 2. As the bridge is symmetrical, piers 1 and 2 have identical results to piers 5 and 4 respectively.

Iter. 1 T_1=0.88s T_2=0.83s	**Piers 1/5**			**Piers 2/4**			**Pier 3**		
	I_{cr} / I_{gr} ratio	Conv.	ρ (%)	I_{cr} / I_{gr} ratio	Conv.	ρ(%)	I_{cr} / I_{gr} ratio	Conv.	ρ(%)
Segm. 1	0.434	87%	1.00	0.524	105%	1.00	0.602	120%	1.00
Segm. 2	0.580	116%	1.00	0.686	137%	1.00	0.686	137%	1.00
Segm. 3	0.550	110%	1.00	0.296	59%	1.00	0.268	54%	1.00
Segm. 4	0.372	74%	1.00	0.244	49%	1.00	0.227	45%	1.00
Segm. 5	0.289	58%	1.00	0.117	23%	1.00	0.096	19%	1.00

Table 2. I_{cr}/I_{gr} ratios and convergence for Iteration 1.

A substantial decrease in the effective flexural stiffness is observed for the sections at the base of the piers. This is due to the small amount of reinforcement still existing in the sections and due to the high effective flexural stiffness at the start of the analysis. The resulting effective stiffness values are inserted into the analysis for Iteration 2, the results of which are presented in Table 3.

Iter. 2 T_1=1.16s T_2=0.91s	**Piers 1/5**			**Piers 2/4**			**Pier 3**		
	I_{cr} / I_{gr} ratio	Conv.	ρ(%)	I_{cr} / I_{gr} ratio	Conv.	ρ(%)	I_{cr} / I_{gr} ratio	Conv.	ρ(%)
Segm. 1	0.565	130%	1.00	0.524	100%	1.00	0.606	101%	1.00
Segm. 2	0.570	98%	1.00	0.653	95%	1.00	0.685	100%	1.00
Segm. 3	0.524	95%	1.00	0.508	172%	1.00	0.514	191%	1.00

Segm. 4	0.352	95%	1.00	0.366	150%	1.00	0.404	178%	1.00
Segm. 5	0.378	130%	1.00	0.321	275%	1.00	0.334	348%	1.00

Table 3. I_{cr} / I_{gr} ratios and convergence for Iteration 2.

During Iteration 2 a shift of the structural period is observed from T_1 = 0.88s to T_1 = 1.16s. The effective flexural stiffness calculated is now much higher than the initial input value for all base sections of all piers. As a result, the analysis is undertaken with forces that correspond to a more flexible structural system in relation to the amount of flexibility that the cross sections can provide. The convergence differences in both iterations clearly demonstrate that with a single calculation there is either an overestimation of seismic forces which would yield an uneconomical reinforcement arrangement and underestimation of displacements, or an underestimation of the seismic forces with a high risk of providing less reinforcement than what is required, and at the same time overestimation of displacements. Therefore, the iteration process to define the boundaries of the effective flexural stiffness values is proven to be very meaningful.

As the iterations continue there are adjustments in the longitudinal reinforcement ratio for the sections that cannot bear the seismic forces. Iterations without increment of reinforcement are also necessary so that the effective flexural stiffness distribution can find an optimum point within the structure. Satisfactory results are obtained when the convergence at each segment is less than 5%. For the bridge example this occurs at Iteration 10 as shown in Table 4.

Iter. 10	**Piers 1/5**			**Piers 2/4**			**Pier 3**		
T_1=0.97s T_2=0.80s	I_{cr} / I_{gr} ratio	Conv.	ρ(%)	I_{cr} / I_{gr} ratio	Conv.	ρ(%)	I_{cr} / I_{gr} ratio	Conv.	ρ(%)
Segm. 1	0.610	100%	2.08	0.531	100%	1.17	0.603	100%	1.17
Segm. 2	0.568	100%	1.00	0.681	100%	1.00	0.686	100%	1.00
Segm. 3	0.523	100%	1.00	0.351	100%	1.00	0.321	96%	1.00
Segm. 4	0.355	100%	1.00	0.276	100%	1.00	0.271	97%	1.00
Segm. 5	0.382	100%	1.64	0.265	100%	1.17	0.268	98%	1.17
Average	*0.488*	-	*1.35*	*0.407*	-	*1.06*	*0.389*	-	*1.04*

Table 4. I_{cr} / I_{gr} ratios, convergence and reinforcement for Iteration 10.

The average value of the ratio in each segment is consistently less the initially assumed value of I_{cr}/I_{gr} = 0.50, therefore economy has been achieved on the provided reinforcement. This is also demonstrated by the shift of the structural period from $T_{1(iteration\ 1)}$ = 0.88s to $T_{1(iteration\ 10)}$ = 0.97s. The average ratio of longitudinal reinforcement for all piers is calculated as ρ_{ave}=1.15%.

Confinement reinforcement for ductile design

As this analysis refers to a force-based design approach, the piers need to be checked for confinement reinforcement in accordance with BS EN 1998-2 Clause 6.2.1. For an axial force at the base of the pier of N_{Ed} = 17.5 MN and a characteristic compressive cylinder strength of f_{yk} = 40 MPa the normalised axial force limit of 0.08 is exceeded as η_k = 0.091. Therefore, confinement reinforcement at potential plastic hinge locations must be provided.

Plastic hinge locations are considered at the top and bottom of each pier. The confinement reinforcement calculation is based on Annex E of BS EN 1998-2 and the same amount is provided for the two sets of longitudinal reinforcement at plastic hinge zones calculated for piers 1/5 and piers 2/3/4 (ratios of ρ = 1.64% and ρ = 1.17% respectively). The confinement stirrups consist of 10mm diameter orthogonal hoops spaced at 125mm c/c. Based on this amount of confinement links, and in accordance with BS EN 1992-2 Section 3 and BS EN 1992-1-1 Clause 3.1.9 the stress-strain relationship of confined concrete is calculated with a cylinder compressive strength of $f_{cd,c}$ = 34.8MPa and a maximum strain of $\varepsilon_{cu2,c}$ = 0.018. The moment-curvature curves for the 1600x3000 (width x depth) pier sections are presented in Figure 4.

By reading from Figure 4 the curvature at yield of reinforcement and at ultimate capacity of the section the curvature ductility can be estimated. The curvature ductility for bending in the transverse direction μ_Φ for piers 1/5 and 2/3/4 is 10.0 and 10.3 respectively. This information is

used later in the calculation of the ultimate displacement at deck level when performing the push over analysis.

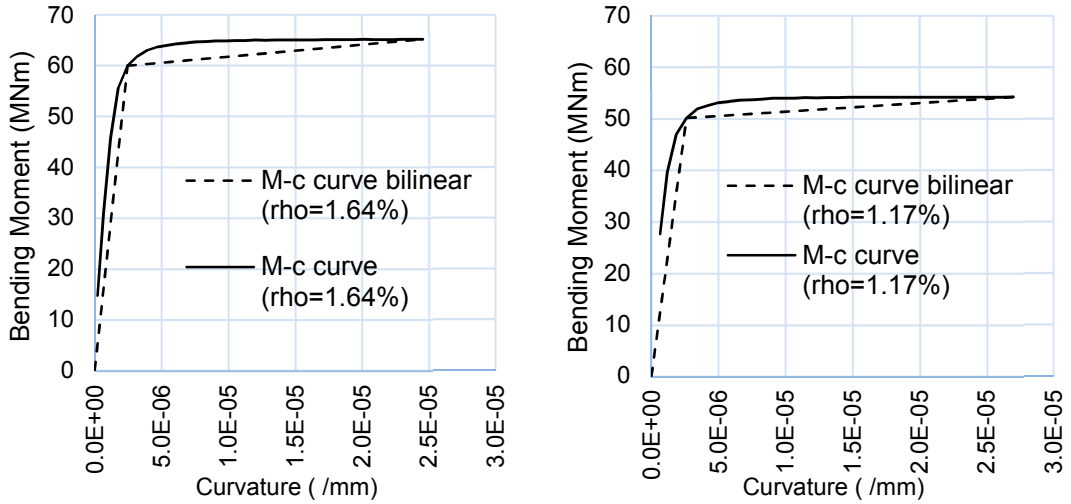

Figure 4: Pier section moment curvature curves at plastic hinges for ρ=1.64% and ρ=1.17%. Cross section 1600 x 3000 (width x depth)

Verification of short pier seismic design in the longitudinal direction

The same effective flexural stiffness is applied at the piers in both horizontal directions. This effective flexural stiffness is calculated from the results converging in the transverse direction. To verify the seismic design in the longitudinal direction the applied longitudinal bending moment *My*=37.7MNm is applied on the relevant cross section (with width = 3.0m and depth = 1.6m) and the I_{cr}/I_{gr} ratio is calculated. The curvature at yield of reinforcement is calculated from a moment-curvature relationship taking into account the confinement reinforcement calculated in the previous section. It has been observed that the maximum bending moment occurs at the top of piers P1/P5. The M-c relationship for the 3000x1600 (width x depth) cross section at this location with longitudinal reinforcement ratio of 2.08% is given in Figure 5.

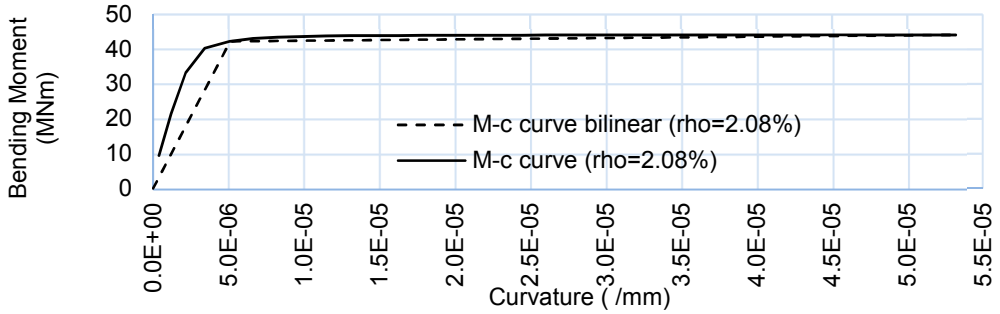

Figure 5: Pier section moment curvature curve at plastic hinges for ρ=2.08%. Cross section 3000 x 1600 (width x depth)

Based on the results of Figure 5 the curvature at yield is $\Phi_y = 5*10^{-6}$ which corresponds to a bending moment value of *My* = 42MNm. Therefore, using the elastic modulus of concrete value of E_c = 35200 N/mm^2, the cracked second moment of inertia is found based on Equation (1) as I_{cr} = 0.238m^4, providing a ratio of I_{cr}/I_{gr} of 0.24. It can be observed that the calculated ratio is substantially lower than the considered in the analysis ratio of 0.61. As a result, the longitudinal direction seismic design for the shorter piers is satisfied in terms of forces. In terms of displacements and for the calculation of the expansion joint gap at the abutments, the analysis may be repeated assigning the calculated I_{cr}/I_{gr} ratio at the top of the short piers, however this calculation is outside the scope of the present study.

Analysis B: Uniform pier effective flexural stiffness

Assumptions

A single analysis is performed based on an average effective flexural stiffness corresponding to an average I_{cr} / I_{gr} ratio of 0.50. This value can be considered as a reasonable first estimate based on the results of Analysis A. A significantly lower value than this, say a value of 0.30, would underestimate the design seismic forces as the structural period would be based on an average effective flexural stiffness much lower than the converged effective flexural stiffness predicted from Analysis A. On the other hand, a significantly higher value would decrease the structural period and as a result increase the seismic forces leading to a disproportionally uneconomical seismic design of the piers.

Analysis results and discussion

The initial reinforcement assumed for the pier sections for Analysis B, is taken from the already known and optimised reinforcement of Analysis A. After undertaking the single analysis, it is found that some of the sections cannot sustain the design seismic forces – as expected – therefore the reinforcement for these sections is increased. The results are tabulated in Table 5 where the resulting effective stiffness and final reinforcement are given.

T_1=0.81s	**Piers 1/5**		**Piers 2/4**		**Pier 3**	
T_2=0.75s	I_{cr} / I_{gr}	ρ (%)	I_{cr} / I_{gr}	ρ (%)	I_{cr} / I_{gr}	ρ (%)
Segm. 1	0.563	2.08	0.536	1.17	0.579	1.17
Segm. 2	0.576	1.00	0.678	1.00	0.689	1.00
Segm. 3	0.457	1.00	0.260	1.00	0.253	1.00
Segm. 4	0.385	1.17	0.262	1.17	0.235	1.17
Segm. 5	0.445	2.08	0.248	1.44	0.228	1.44
Average	*0.485*	*1.47*	*0.369*	*1.13*	*0.343*	*1.10*

Table 5. I_{cr} / I_{gr} ratios after analysis with initial I_{cr} / I_{gr} = 0.50 and final reinforcement for piers

Analysis B predicts an average longitudinal reinforcement ratio between all piers of ρ_{ave} = 1.23%. In relation to Analysis A, the longitudinal reinforcement has increased by 7%. This corresponds approximately to 161 tons of extra steel reinforcement for the bridge example.

In addition, Analysis B would predict transverse displacements at deck level corresponding to a ratio of I_{cr}/I_{gr} of 0.50, which is substantially higher than the predicted in the analysis even with the higher reinforcement assigned. This underestimation of displacements for the examined bridge example may not be that critical to review introduced P-Δ effects, however for higher displacement values these effects may be significant. From an analysis using a uniform effective flexural stiffness P-Δ effects may be missed.

Analysis C: Push-over analysis

Background and assumptions

The purpose of Analysis C is to demonstrate that a meaningful push over analysis can be undertaken using the effective flexural stiffness values at the base of the piers predicted in Analysis A, as well as to validate its findings. This displacement-based design approach uses a structure substitute system represented by an inverted pendulum which describes the behaviour of the cantilever piers.

The push-over calculation is described analytically in Priestley et al. (1996). An initial transverse yield displacement Δ_y is assumed at deck level and then the total displacement is calculated from the available plastic hinge rotation capacity at pier base. The total target displacement is used to calculate the effective period of the system and from there, the effective stiffness is calculated. The equation from the Takeda model is used to calculate the effective damping from the assumed total design displacement, and the available displacement ductility. The equivalent seismic force F_u at ultimate is calculated by multiplying the effective stiffness with the total displacement and then the force at yield F_n is estimated from the bilinear relationship with the ultimate force F_u. Based on the elastic deformation (Δ_y) that force F_n can cause to the system, the initial assumption for the yield displacement is verified.

The analysis is undertaken for each pier separately, however the first transverse fundamental mode shape is simulated assuming that all piers deform simultaneously and in the same direction. The plastic hinge rotation is selected so that the deformation at deck level approximately matches the deformation of the first structural mode shape of Analysis A.

Displacement Spectrum

The displacement spectrum is based on the horizontal elastic response spectrum by converting the acceleration ordinates to displacement ordinates as described in Clause 3.2.2.2 (5)P of BS EN 1998-1. The long-period transition structural period T_D is given in BS EN 1998-1 with a value of 2s. For the displacement spectrum, that means that beyond this period there is a constant displacement value. Even though this may be a reasonable assumption for buildings, for long structural period structures such as bridges a higher value for the corner period (period at which the displacement becomes constant) would seem to provide more appropriate results. Therefore, for the displacement-based design exercise herein, a corner period of T_D = 4s is adopted. The selection of this value is in line with the provided displacement spectrum in Priestley et al. (2007) as well as with the discussion of recent work from Kappos et al. (2012). In fact, the elastic acceleration spectrum given in Priestley et al. (2007) for firm soil that is used to calculate the displacement spectrum is identical with the elastic acceleration spectrum of BS EN 1998-1 for soil Type B (T_B = 0.15s and T_C = 0.5s) except from the value of the period T_D. The acceleration and displacement spectra for piers 1 to 3 are shown in Figure 6.

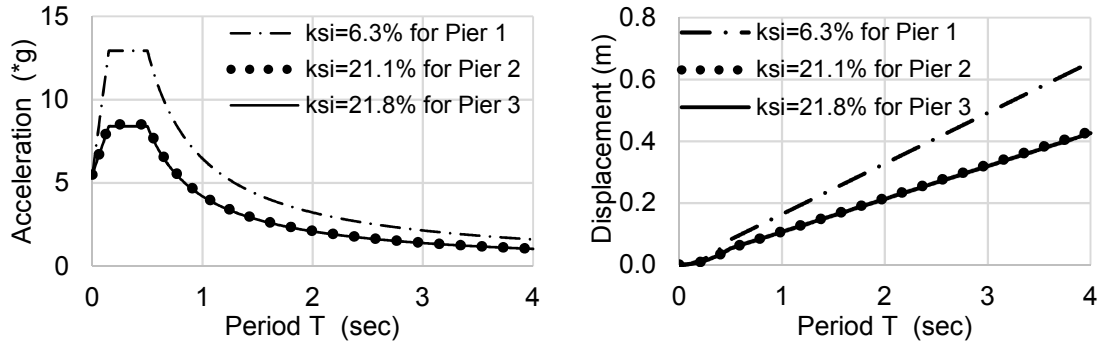

*Figure 6: Elastic horizontal acceleration and displacement spectra for push-over analysis with PGA = 1.3*0.36g and for soil Type B*

Analysis results and discussion

The analysis results are presented in Table 6. Each column in the table contains the results of a single pier push-over analysis.

Calculation step	**Parameter and formula**	**Units**	**Pier 1/5**	**Pier 2/4**	**Pier 3**
Assumed initial yield displacement	Δ_y	m	0.100	0.040	0.049
Yield rotation at pier base	$\theta_y = \Delta_y / L$	rad	0.010	0.003	0.003
Plastic hinge length	$L_p = 0.08L + 0.022 f_{yk} d$ (d: bar dia, taken as 25mm)	m	1.2	1.3	1.6
Available plastic hinge rotation	$\theta_p = \varphi_u / \varphi_y$ (from M-c curve, see Fig. 4)	rad	0.025	0.031	0.038
Plastic hinge rotation at mode shape	$\theta_{p,design}$	rad	0.001	0.019	0.023
Displacement due to plastic hinge rotation	$\Delta_p = \theta_{p,design} \times L$	m	0.010	0.232	0.371
Total displacement	$\Delta_d = \Delta_y + \Delta_p$	m	0.110	0.272	0.420
Displacement ductility	$\mu_d = \Delta_d / \Delta_y$	-	1.1	6.8	8.6

Effective damping (Takeda model)	$\xi_{eff} = 0.05 + \frac{\left(1 - \frac{0.95}{\sqrt{\mu_d}} - 0.05\sqrt{\mu_d}\right)}{\pi}$	-	0.063	0.211	0.218
Effective period	T_{eff} from displacement spec. Fig. 6	sec	0.670	2.520	3.940
Effective stiffness	$K_{eff} = 4\pi^2 \frac{M}{T_{eff}^2}$	N/m	1.38E+08	9.76E+06	3.99E+06
Force at ultimate	$F_u = K_{eff} \times \Delta_d$	kN	15186	2656	1675
Force at yield	$F_n = \frac{F_u}{r \times \mu_d - r + 1}$, r = 0.05	kN	15111	2059	1215
Moment of inertia ratio	$\frac{I_{cr}}{I_{gr}}$ from Analysis A	-	0.382	0.265	0.268
Effective flexural stiffness	$K_{cr} = 3 \times E \times \frac{I_{cr}}{L^3}$	N/m	1.45E+08	5.16E+07	2.49E+07
Period at effective flexural stiffness	$T_{cr} = 2 \times \pi \times \sqrt{\frac{M}{K}}$	sec	0.65	1.10	1.58
Calculated displacement from F_n	$\Delta_y' = F_n / K_{cr}$	m	0.104	0.040	0.049
Ratio of yield displacement	$Ratio = \Delta_y' / \Delta_y \times 100$	-	104%	100%	100%

Table 6. Push-over analysis for each pier

Table 6 provides useful information for the comparison with the results of Analysis A. It is observed that at approximately the maximum displacement of the first transverse mode shape, the more heavily reinforced piers 1 and 5 behave for most of the design displacement in an elastic fashion and as a result they contribute marginally to the damping of the overall system. On the other hand, piers 2, 3 and 5 accommodate a substantially higher plastic hinge rotation and therefore they contribute substantially more to the overall damping. The average values of the displacement ductility and the effective flexural stiffness structural period among all five piers are μ_d = 4.9 and T_{cr} = 1.02s. It is noted that this average value of structural period of the independent single degree of freedom systems is very close to the first structural period of Analysis A (T_1 = 0.97s).

From recent work from the authors, Gren et al. (2018), for irregular viaducts much higher displacement ductility values were observed when performing non-linear response analysis allowing plastic hinge formation at the base of piers in the transverse direction. Therefore, the calculated in the present analysis average displacement ductility value is deemed to be a realistic, lower bound value for an inelastic design. Moreover, the average displacement ductility value provides a very good verification for the behaviour factor of q = 3.5 used in the force-based design approach of Analysis A. As proposed in Chopra (2007) for longer structural periods of approximately 1s and beyond, the response reduction factor in inelastic design spectra (R, or q in BS EN 1998-1 terminology) can be taken as equal to the displacement ductility μ_d. As a result, the push-over analysis provides meaningful results on the bridge example and demonstrates that the calculated I_{cr} / I_{gr} values provide an indication on the amount of plastic hinge rotation and as a result energy dissipation of the overall system.

The performance curves of piers 1, 2 and 3 are plotted on the acceleration-displacement demand curves as shown in Figure 7.

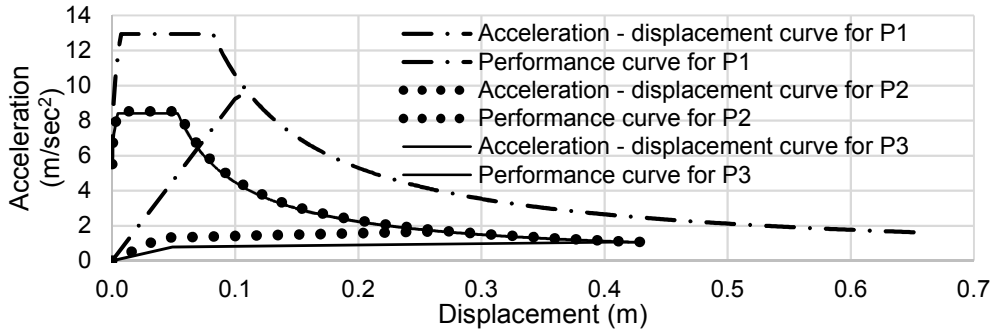

Figure 7: Performance curves of piers 1, 2 and 3 from push-over analysis

Summary and conclusions

A numerical analysis approach has been discussed with aim to optimise the seismic design forces of irregular bridges with monolithic concrete piers, where bearings want to be avoided for shorter piers that attract more seismic loading. The approach was illustrated by an example of a typical irregular bridge, but it largely fits other bridge geometries. The analysis approach incorporates the calculation of the effective flexural stiffness at several locations along the piers and at each pier separately. The analysis results are compared with the results of a similar analysis with a uniform value of effective flexural stiffness, typically undertaken during design. Finally, the results are also compared with the results of a push-over analysis.

For the presented case a significant reduction in the required amount of pier longitudinal reinforcement has been found due to the optimisation of the seismic forces from the analysis of piers allowing for cracking. Even though a specific value on the reduction is difficult to be based from a single irregular bridge geometry, the saving in the pier longitudinal reinforcement is expected to be in the order of at least 5% in relation to a standard analysis with uniform effective flexural stiffness. Moreover, the converged I_{cr}/I_{gr} ratios provide a more accurate calculation of the seismic displacements. This is of vital importance for the calculation of P-Δ effects.

The benchmarking of the analysis results with the results of the push-over analysis reveal that the different cracked properties at the pier bases drive the dissipation of energy in the overall system and provide an indication of which piers are likely to absorb more energy. The piers with the lower I_{cr}/I_{gr} ratios are eventually accommodating larger displacements and are contributing more to the damping of the system.

References

BS EN 1998-1:2004+A1:2013, *Eurocode 8: Design of structures for earthquake resistance – Part 1: General rules, seismic actions and rules for buildings*, AMD 31st May 2013

BS EN 1998-2:2005+A2:2011, *Eurocode 8: Design of structures for earthquake resistance – Part 2: Bridges*, AMD 29th February 2012

BS EN 1992-1-1:2004+A1:2014, *Eurocode 2: Design of concrete structures – Part 2: Concrete bridges – Design and detailing rules,* AMD 28th February 2008

BS EN 1992-2:2005, *Eurocode 2: Design of concrete structures – Part 1-1: General rules and rules for buildings,* AMD 31st July 2015

Priestley MJN, Seible F NS Calvi GM (1996), *Seismic Design and Retrofit of Bridges*, New York: John Wiley & Sons, Inc.

Priestley MJN, Calvi GM and Kowalsky MJ (2007), *Displacement-based Seismic Design of Structures*, Pavia, Italy: IUSS PRESS

Chopra AK (2007), *Dynamics of Structures – Theory and Applications to Earthquake Engineering*, Third Edition, Upper Saddle River, New Jersey, Pearson Prentice Hall

Kappos AJ, Gidaris IG, Gkatzogias KI (2012), *Problems associated with direct displacement-based design of concrete bridges with single-column piers, and some suggested improvements*, Bulletin of Earthquake Engineering, 10(4), pp. 1237-1266

Gren SM, Karamichalis N, Hansen JE (2018), *Elastic and inelastic seismic design of an irregular bridge in Kashmir, India*, 16th ECEE, 18-21 June 2018

SOFiSTiK Manual (2016), Version 2016, SOFiSTiK AG, Oberschleissheim, Germany